Proceedings of the 8th World Congress on Mechanical, Chemical, and Material Engineering (MCM'22)
Prague, Czech Republic – July 31, 2022 - August 02, 2022
Paper No. HTFF 150
DOI: 10.11159/htff22.150

Simultaneous Heat and Moisture Transport in 3D Printed Walls

Andrea Fragnito[1], Marcello Iasiello[1], Gerardo Maria Mauro[2], Costantino Menna[3]
[1]University of Naples, Department of Industrial Engineering
Piazzale Tecchio, Napoli, Italy
andrea.fragnito@unina.it; marcello.iasiello@unina.it
[2]University of Sannio, Department of Engineering
Piazza Roma, Benevento, Italy
germauro@unisannio.it
[3]University of Naples, Department of Structures for Engineering and Architecture
Via Claudio, Napoli, Italy
costantino.menna@unina.it

Abstract - The national and international building stock – representing one of the most intensive energy-consuming sectors worldwide – is characterized by a large share of old constructions, designed without following any energy criteria. This scenario has promoted the rising of powerful technologies, *e.g.,* Additive Manufacturing (AM), which despite its recent rise is leading the innovation process involving both the industrial and civil sectors. 3D printing techniques are going to outperform current production techniques because of their various advantages, *i.e.,* design of complex forms, uniform materials, reduced production steps and costs. The aim of the present work is to combine the accuracy of computer-aided design (CAD) for AM structures with the benefits of the computational thermo-fluid dynamic simulation (CFD) to perform thermal and moisture performance analysis of innovative building walls. Natural convection and radiation problem – involving buoyancy-driven flow in a cavity – is investigated and solved under appropriate boundary conditions defined in a finite element commercial code. After validation with international guidelines and literature data, the model is simulated in Napoli (Italy) under winter design conditions. Moreover, this work provides a comparison between a simplified procedure for the condensation risk detection, *i.e.,* the Glaser method, and an advanced one – based on the steady-state diffusion theory – which considers latent heat effect and capillary transport of moisture liquid. The results show that the radiative heat transfer mechanism has a significant influence on thermal transmittance. On the other hand – with reference to the case study – here we present the discrepancy between the prediction of the condensation effect during the winter months by adopting the present method with respect to the Glaser one.

***Keywords*:** heat and moisture, 3D printed wall, fluid dynamics, condensation risk, thermal transmittance

1. Introduction

Additive Manufacturing (AM) or 3D printing is a process aimed at the construction of a final part (components, semi-finished or finished products) through the addition of consecutive layers of material. This purpose is in contrast with subtractive manufacturing – the operating principles of many traditional production techniques – which achieves solid components by removing undesired material (turning, milling, etc.). From a technological point of view, AM should not be regarded as a recent innovation. The birth of 3D printing can be referred to mid-80s with the introduction of rapid prototyping (RP). Since then, great progress has been made, managing to print small objects – on the micrometre scale – and using multiple materials *i.e.,* plastic, metal, ceramic, wax, composite materials, and concrete. The chances for testing and adopting this technology are significantly increased, resulting in the reduction of production times compared to the past. In the early 2000s complex ceramic parts were provided by using stereolithography or Contour Crafting (CC) techniques [1]. Differently from Contour Crafting, freeform construction is focused on the manufacture of full-scale construction components *e.g.,* panels and walls. This process, also mentioned as "Concrete Printing" (CP), appeared in 2007 [2]. However, the Concrete Printing technology has been developed to retain 3D freedom and has a smaller resolution of deposition, which allows for greater control of internal and external geometries. Therefore, with the fast development of high precision instruments for 3D printing, innovative building walls are investigated extensively in recent years [3], [4]. However, problems linked to thermal management, *i.e.,* thermal insulating enhancement, and hygrothermal performance have not been further deepened.

This study aims to contribute to the knowledge gap-filling on thermal analysis of 3D printing techniques for building elements prototyping, defining reliable predictions useful for thermal optimization and moisture management issues. Great attention has been posed to the modalities to increase the thermal performance of envelopes but practically no evidence has been dedicated to the study of condensation for AM building elements. Since moisture condensation is one of the main causes that produce negative effects on the behaviour of traditional building envelopes in terms of deterioration of materials, increasing of the thermal conductivity of the insulation, weakening of structures, growth of mold and mildew [5], the aim is to investigate both the occurrence of condensation and the thermal behaviour under the most critical conditions. In this regard – performing the analysis on Naples (South Italy, Mediterranean climate) winter design conditions – we present the value of the thermal transmittance for the considered prototype, to be lower than the limit value of 0.36 W/m^2K, imposed for this climatic zone by the Italian ministerial decree DM 26/6/2015 [6]. Moreover, since the limitations of the Glaser method are well-known [7], we firstly provide the results of the moisture problem applying the former, and then we underline the overestimation effects comparing it with the present study model. The aim is to detect if this kind of geometries can be affected to mold and deterioration.

2. Problem formulation

The evaluation of the thermal and hygrometric performance of the 3D printed wall is divided into 3 different studies: buoyant flow, radiative heat transfer (non-isothermal flow) and moisture transport (in building materials, in the air) in confined cavities. All these points are achieved simultaneously because of their mutual influence, as depicted in Fig. 1.

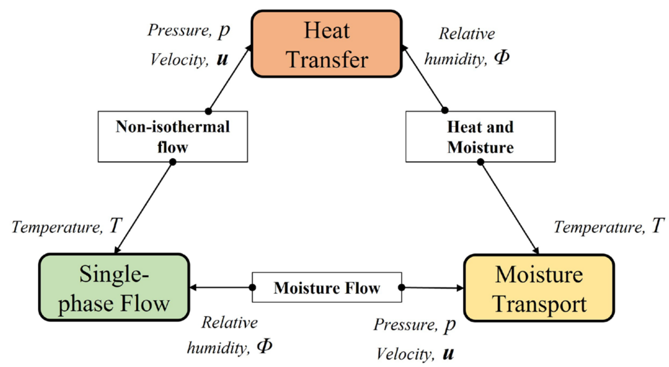

Fig. 1: Problem definition.

2.1. Case study

Among the several benefits of 3D printing techniques, one of the most relevant is the design of low-weight structures, which results in the presence of air gaps. Leaving an air gap between two layers in a wall allows the air to be poor heat conductor, responding as a barrier to heat transfer. Free convection is typically the main driving force of the resulting recirculating flow. Different approaches have been developed, starting from using the Boussinesq approximation and variable viscosity, while performing a linearized approach and reported results for moderate Rayleigh numbers [8]. The problem under consideration is depicted schematically in Fig. 1.

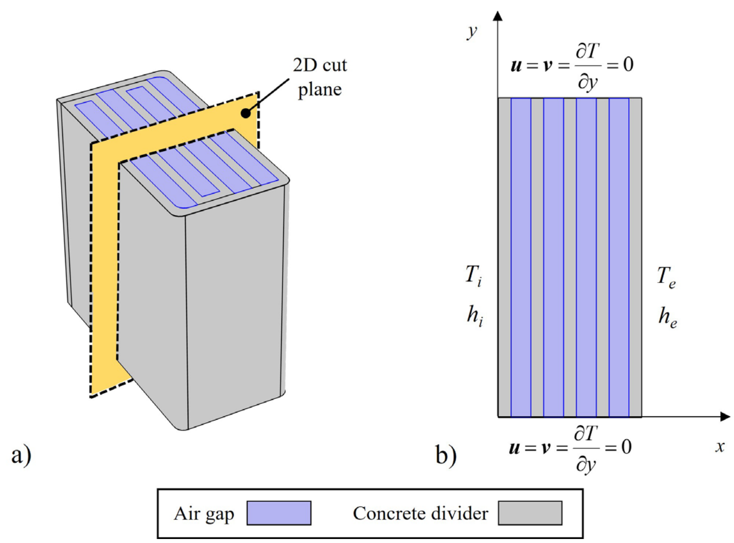

Fig. 2: Problem model: a) 3D sample; b) 2D section.

The flow domain is the interior of a 2D rectangular cavity with a fixed aspect ratio. The horizontal surfaces of the cavity are assumed to be perfectly adiabatic, while the vertical walls are surrounded by air so that convective heat flux is assigned. Parameters T_i, h_i and T_e, h_e are temperatures and convective heat transfer coefficients for internal and external environment, defined for the left and right walls, respectively. Owing to heat transfer through the vertical walls, density changes result in a recirculating flow, in a range where the flow remains in a laminar regime. To perform a comparison of the evaluation methods, the moisture problem is modelled according to the EN ISO 13788 [7] standards. Thus, the methodology is applied for the design of a building envelope prototype for the winter climatic conditions of Naples, which corresponds to an outer temperature $T_e = 2$ °C and $\phi_e = 92\%$, and an inner temperature $T_i = 20$ °C, with $\phi_i = 55\%$. So, the simulations are performed under a temperature difference of 18 °C. In the hypothesis of stationary flow, elements with a simple flat geometry – made from a sequence of homogeneous and isotropic layers, including air layers – and isothermal surfaces outside the wall, thermal transmittance is a regulated parameter to evaluate the thermal performance [9]:

$$U = \frac{1}{\frac{1}{h_i} + \sum_{i=1}^{n} \frac{s_i}{k_i} + \sum_{j=1}^{m} R_j + \frac{1}{h_e}} \tag{1}$$

The evaluation of the convective coefficients h_i and h_e is achieved from UNI EN ISO 6946 [9], which specifies the conventional values of surface resistance. Indeed, for the external convection the air velocity is assumed to be 4 m/s [8]. Since transition in a free convection boundary layer depends on the relative magnitude of the buoyancy and viscous forces in the fluid, a parameter used to compare the thermal gradient with the viscous resistance is the dimensionless Rayleigh number, which is the product of the Grashof and Prandtl numbers and measures the ratio of the buoyancy forces with respect to the viscous forces:

$$Ra = Gr \cdot Pr = \frac{g\beta(T_S - T_\infty)L^3}{\nu\alpha} \tag{2}$$

Where L is the characteristic length, *i.e.,* the height. Depending on the Rayleigh number the flow can be categorized as turbulent or laminar [10]. For rectangular enclosures, Rayleigh numbers less than 10^8 indicate a buoyancy-induced laminar flow, with the transition to turbulence occurring over the range of $10^8 < Ra < 10^{10}$ [11].

2.2. Governing equations

To solve the non-isothermal flow – which occurs in natural convection problems – the Boussinesq approximation performed. The unknown parameters that appear in the following equations are the fluid velocity vector $\boldsymbol{u}$, the pressure and the temperature *T*:

$$\nabla \cdot \boldsymbol{u} = 0 \tag{3}$$

$$\rho(\boldsymbol{u} \cdot \nabla \boldsymbol{u}) = -\nabla p + \mu \nabla^2 \boldsymbol{u} - \rho\beta(T - T_0)\boldsymbol{g} \tag{4}$$

$$\rho c_p (u \cdot \nabla T) = \nabla \cdot (k \nabla T) \tag{5}$$

Where, ρ is the fluid density, μ the fluid dynamic viscosity, β the coefficient of thermal expansion, k the thermal conductivity, c_p the specific heat at constant pressure, $\boldsymbol{g}$ the acceleration due to gravity, and T_0 the reference temperature.

As regards the coupling between heat and moisture transport through the building material, the equations implemented in this study are here presented, under the hypothesis of steady-state flow, 2D model, thermophysical properties dependent on temperature, absence of heat and moist sources, in accordance to the European Standard EN 15026 [12]:

$$-\nabla \cdot \left(k_{eff} \nabla T + L_v \delta_p \nabla(\Phi p_{sat})\right) = 0 \tag{6}$$

$$\nabla \cdot \left(-\xi D_W \nabla \Phi - \delta_p \nabla\left(\Phi p_{sat}(T)\right)\right) = 0 \tag{7}$$

Where k_{eff} is the effective thermal conductivity, L_v is the latent heat of evaporation, δ_p is the vapor permeability, Φ is the relative humidity, p_{sat} the vapor saturation pressure, ξ is the moisture storage capacity, D_W is the moisture diffusivity. For moist air, heat transfer and moisture transport – by diffusion and convection – are modelled through the following equations:

$$\rho c_p \boldsymbol{v} \cdot \nabla T + \nabla \cdot \boldsymbol{q} = 0 \tag{8}$$

$$M_v \boldsymbol{v} \cdot \nabla c_v + \nabla \cdot \boldsymbol{g}_v = 0 \tag{9}$$

$$\boldsymbol{g}_v = -M_v D \nabla c_v \tag{10}$$

Where M_v is the molar mass of water vapor and *D* is the vapor diffusion coefficient in air. For the thermal radiation problem, the surface-to-surface model is implemented, where each wall of the cavity is opaque to thermal radiation – the emissivity of cementitious materials is equal to 0.9 – and the fluid is deemed to be transparent and not participating in radiative heat transfer.

2.3. Glaser Method

The Glaser method consists of the detection of water condensation inside or on building materials surfaces, through a graphic comparison between the saturation pressure and the partial steam pressure. The building envelope, dividing environments with different temperatures and relative humidity, is subject to heat and moisture transfer, which is caused by the difference between the vapor partial pressure of the two environments – determined by Eq. 11 – and by the wall vapor permeability.

$$p_{vap}(\varphi, T) = \varphi \cdot p_{sat}(T) \tag{11}$$

Condensation should occur if $p_{vap} = p_{sat}(T)$, where the distribution of partial pressure of vapour is determined by means of the Fick's law. By neglecting heat and moisture storage, latent heat effect and capillary transport of liquid moisture, the following equations are obtained for heat and moisture transport:

$$\nabla \cdot \left(k_{eff} \nabla T\right) = 0 \tag{12}$$

$$\nabla \cdot \left(\delta_p \nabla\left(\Phi p_{sat}(T)\right)\right) = 0 \tag{13}$$

Moreover, the Glaser method does not consider some important physical phenomena, *e.g.,* the dependence of thermal thermal conductivity on the moisture content, the variation of the properties of the materials as a function of the moisture content, the air flows through cavities, and therefore it generally overestimates the condensation risk. Concerning the materials, the cementitious mortar for AM is a composite material ready-to-use, developed to meet the needs of the user who tends to realize manufactured goods using 3D extrusion technologies. This material is a premixed product with selected sands and specific components which guarantee the mortar to be self-sustaining during printing, maintaining the shape required by the starting 3D model, and at the same time ensuring excellent workability and progressive development of mechanical resistances [13]. The fresh mortar density is 2150 kg/m^3, while the hardened one is 2000 kg/m^3. For CFD simulation purposes, the last parameter to be determined – and above all one of the most influential for evaluating the thermal performance of the model – is the thermal conductivity. In this regard, through an experimental test, the thermal conductivity of the cementitious mortar under investigation has been evaluated. The investigations have been carried out in the Insulating Material Thermal Analysis Laboratory (IMATlab) of the University of Naples Federico II. The NETZSCH Guarded Hot Plate (GHP) 456 Titan® system has been employed to perform absolute thermal conductivity measurements on cementitious mortar samples geometrically defined by a square section of side 30 cm. It works with sheeted individually calibrated PT100 resistance temperature sensors (resolution 1 mK, accuracy in the range of a few 10 mK). The experimental analysis – for a setpoint temperature of 10 °C – returns a conductivity value (k) equal to 1.2 W/m K. Based on this value and on the governing equations, the thermophysical properties implemented in the FEM model are listed in Tab. 1.

Table 1: Thermophysical properties.

Cementitious mortar properties	**Value**
Density, ρ (kg/m^3)	2000 kg/m^3
Specific heat, c_p (J/kg K)	880 J/(kg K)
Water content, w (kg/m^3)	$w = \frac{146}{(1 + (-8 \cdot 10^{-8} \cdot R_{H_2O} T_{ref} \rho_w \ln(\Phi)^{1.6})^{0.375}}$
Thermal conductivity, k_{eff} (W/m K)	$k_{eff} = 1.2 + \frac{12.64}{1000} w$
Vapour permeability, δ_p (kg/(m s Pa))	$\delta_p = f(w(\Phi))$
Moisture diffusivity, D_w (m^2/s)	$D_w = f(w(\Phi))$

2.4. Grid independence

A well-tuned mesh is needed to capture the solution, especially the temperature and velocity changes near the walls. COMSOL Multiphysics® provides 9 levels of mesh *i.e.,* from extremely fine (1) to extremely coarse (9). The full mesh, extremely fine (1), consists of 97580 tetrahedral elements. To reduce the computational burden, a grid independence test is performed on the thermal transmittance value (*U*), as in Fig. 3. The final mesh level, *i.e.*, finer (as in Fig. 3), represents a compromise between the thermal transmittance value, the percentual deviation and the running time. To validate the results obtained by the simulations, standard values of transmittance are calculated, using the method provided by international regulation (ISO 6946:1996, 1996). The validation approach must be referred to cavity thicknesses less (or equal) than 30 cm. Indeed, the enclosure thickness is assumed to be 10 cm. The transmittance value obtained is 2.3904 W/m^2 K, against the 2.3998 W/m^{2}K of ISO 6946. To verify the model built in COMSOL Multiphysics®, a numerical study on the assessment of thermal transmittance of hollow concrete blocks has been selected as reference work [14]. The mentioned study solves the natural convection problem of two parallel isothermal walls at different temperatures. Both the cases – with and without radiation – are considered, to be evidence of how the percentage deviation is amplified including the radiation.

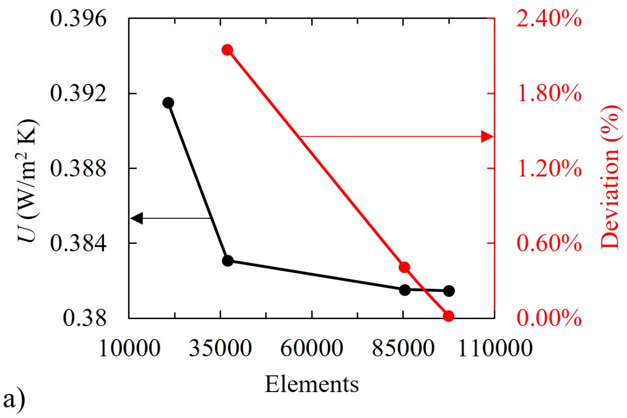

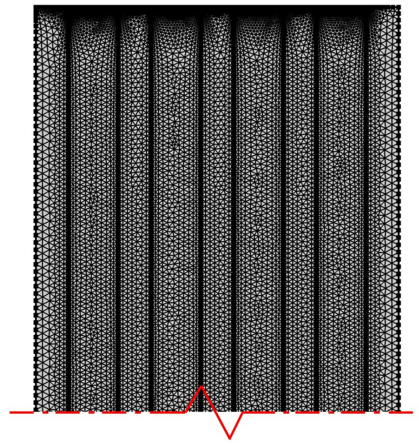

Fig. 3: Grid independence: a) test on thermal transmittance; b) final mesh configuration.

As itemised in Tab. 2., the model results are quite the same for the case without radiation, while a higher (but still limited) difference outcomes from the second case, which accounts for air contribution as participating media for radiative heat transfer through discrete ordinate method (DOM).

Table 2: Comparison between present work and reference thermal transmittance.

Study	**Thermal transmittance, *U* (W/m^{2}K)**	
	No-radiation	DOM
Present work	2.898	5.7
Reference [64]	2.895	5.85
Difference (%)	0.1	2.56

3. Results and discussion

This section is devoted to the comparison between the Glaser method application and the thermo-fluid dynamic one. Specifically, a first comparison between the Glaser Method results for the 1D case and the 2D CFD model with the same assumptions, *i.e.,* 2D simplified, is assessed. Then, the Glaser method limitations are exhaustively highlighted. Moreover, a brief comment on the thermal transmittance is here provided. Thus, as starting point, results are presented in terms of temperature distribution (Fig. 4a), and comparison between the trends of saturation pressure vs partial pressure over the geometry previously described (Fig. 4b). In detail, the diagrams have been obtained implementing Eq. (9) for partial vapour pressure, and saturation pressure (p_{sat}) is evaluated following the EN ISO 13788 standard. Fig. 4 shows that the saturation pressure is linear in the 1D case, while it is affected by the recirculating flow inside cavities in the 2D case. Nevertheless, values at the interfaces are almost equal. Moreover, the slope of the curves does not match perfectly in the concrete region because of the definition of the effective thermal conductivity, dependent on the water content (see Tab. 2). As concerns the partial vapour pressure – since the Glaser method considers the vapour transport in the building materials only by diffusion – the small deviations between the curves in the concrete regions are influenced by the vapor permeability trend. The higher δ_p, the lower the water content, which increases from left to right according to the boundary conditions.

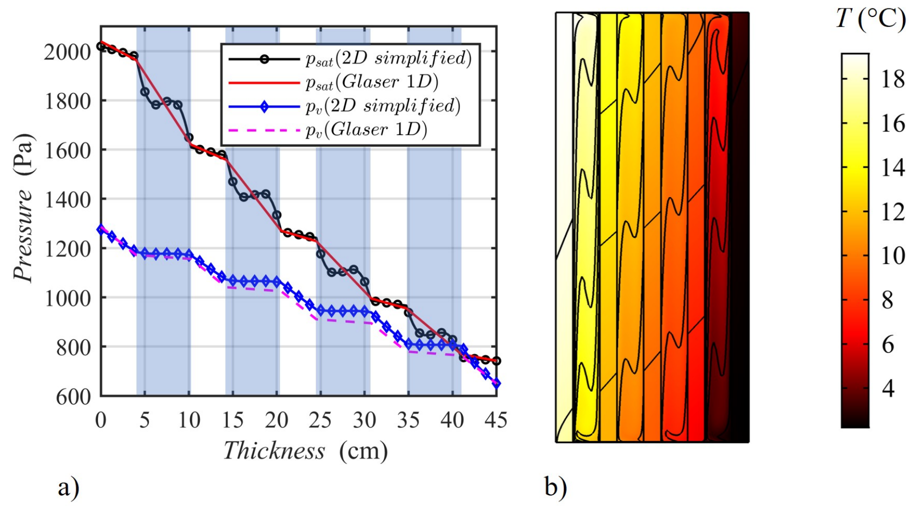

Fig. 4: a) Comparison of saturation and partial pressure between Glaser 1D and 2D simplified model; b) 3D wall temperature field.

Therefore, the 2D trend is a flatter on the left compared to those on the right. At this stage, we consider the results of the model with the contribution of latent heat and, specifically, the transport of moisture by capillarity within the concrete layers. Diagrams in Fig. 5 show the trends of p_{sat} and p_v obtained at first for the model with Glaser method limitations, then without it, *i.e.,* 2D complete.

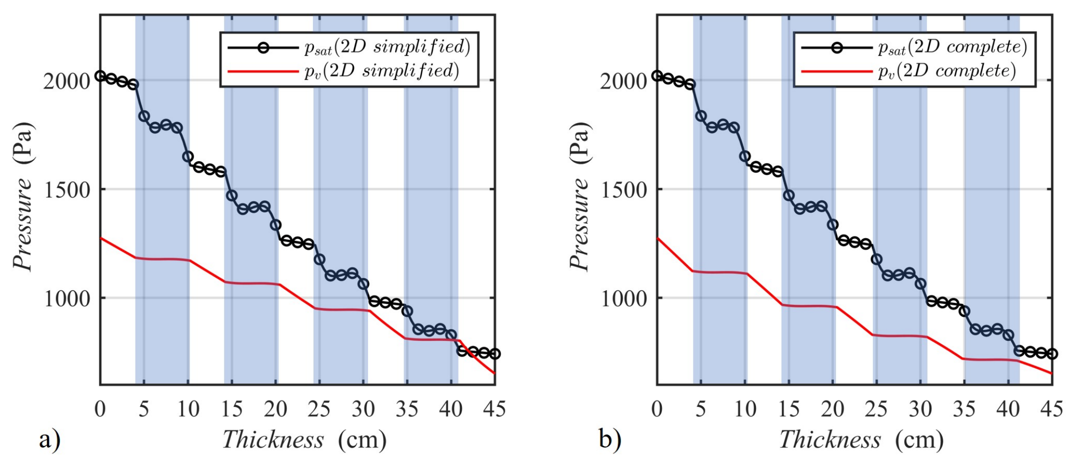

Fig. 5: Difference between condensation risk detection of: a) 2D simplified model; b) 2D complete model.

Based on pure observation – under the tested environmental conditions – interstitial condensation occurs adopting the hypothesis of the Glaser method, as confirmed by the intersection between the partial pressure of vapour and the saturation pressure. Conversely, it does not occur when we consider the contribution of latent heat and the moisture transport by capillary suction – which is quite relevant for high relative humidity values – and depends on the moisture diffusivity. Results provide new useful insights on the use of combined heat and moisture models for the detection of condensation risk, which can be applied to any type of 3D wall that has alternating layers of air and concrete thanks to the accurate CFD approach. By examining different geometries of internal patterns, one should minimize the heat transfer while keeping the maximum partial pressure on the air side constant.

4. Conclusions

In this work, various approaches of modelling heat and moisture transport are assessed with reference to a case 3D printed wall as building envelope. Thermal characteristics, *i.e.,* thermal transmittance and cementitious mortar conductivity, are firstly assessed. Since these walls generally comprise air gaps, the simultaneous influence of buoyant radiative heat transfer and moisture transport (in building materials, in the air) in confined cavities is considered. The to provide a comparison between three models: the simplified procedure for the condensation risk detection, *i.e.,* the Glaser method, the 2D numerical one developed under the same assumptions, *i.e.,* 2D simplified, and an advanced one – based on the steady-state diffusion theory – which considers latent heat effect and capillary transport of moisture liquid, according to the EN ISO 13788 standards. The latter two are modelled through a finite element code. Results, presented in terms of pressure profiles, attest that water content and vapour permeability cause slight differences when comparing the 1D Glaser method and 2D simplified profiles. Differently from the Glaser method – which overestimates the condensation risk – the 2D complete model proves the absence of that issue, thanks to the contribution of latent heat and the moisture transport by capillary suction.

References

[1] B. Khoshnevis, "Automated construction by contour crafting—related robotics and information technologies," *Autom. Constr.*, vol. 13, no. 1, pp. 5–19, Jan. 2004, doi: 10.1016/j.autcon.2003.08.012.

[2] R. A. Buswell, R. C. Soar, A. G. F. Gibb, and A. Thorpe, "Freeform Construction: Mega-scale Rapid Manufacturing for construction," *Autom. Constr.*, vol. 16, no. 2, pp. 224–231, Mar. 2007, doi: 10.1016/j.autcon.2006.05.002.

[3] J. Sun, J. Xiao, Z. Li, and X. Feng, "Experimental study on the thermal performance of a 3D printed concrete prototype building," *Energy Build.*, vol. 241, p. 110965, Jun. 2021, doi: 10.1016/j.enbuild.2021.110965.

[4] T. Pastore, C. Menna, and D. Asprone, "Bézier-based biased random-key genetic algorithm to address printability constraints in the topology optimization of concrete structures," *Struct. Multidiscip. Optim.*, vol. 65, no. 2, p. 64, Feb. 2022, doi: 10.1007/s00158-021-03119-3.

[5] C. Xu, S. Li, and K. Zou, "Study of heat and moisture transfer in internal and external wall insulation configurations," *J. Build. Eng.*, vol. 24, p. 100724, Jul. 2019, doi: 10.1016/j.jobe.2019.02.016.

[6] *D.M. 26/6/15 "Applicazione delle metodologie di calcolo delle prestazioni energetiche e definizione delle prescrizioni e dei requisiti minimi degli edifici."*

[7] *UNI EN ISO 13788:2013 "Hygrothermal performance of building components and building elements - Internal surface temperature to avoid critical surface humidity and interstitial condensation - Calculation methods."*

[8] A. Rubel and F. Landis, "LAMINAR NATURAL CONVECTION IN A RECTANGULAR ENCLOSURE WITH MODERATELY LARGE TEMPERATURE DIFFERENCES," in *Proceeding of International Heat Transfer Conference 4*, 1970, pp. 1–11. doi: 10.1615/IHTC4.3530.

[9] "ISO 6946:1996 (1996) Building components and building elements—thermal resistance and thermal transmittance—calculation method."

[10] D. Saury, N. Rouger, F. Djanna, and F. Penot, "Natural convection in an air-filled cavity: Experimental results at large Rayleigh numbers," *Int. Commun. Heat Mass Transf.*, vol. 38, no. 6, pp. 679–687, Jul. 2011, doi: 10.1016/j.icheatmasstransfer.2011.03.019.

[11] Y. Liu and H. Huang, "Effect of three modes of linear thermal forcing on convective flow and heat transfer in rectangular cavities," *Int. J. Heat Mass Transf.*, vol. 147, p. 118951, Feb. 2020, doi: 10.1016/j.ijheatmasstransfer.2019.118951.

[12] "UNI EN 15026:2008 'Hygrothermal performance of building components and building elements - Assessment of moisture transfer by numerical simulation.'"

[13] "https://www.italcementi.it/it/tecnologia-3d-printing."

[14] G. Henrique dos Santos, M. A. Fogiatto, and N. Mendes, "Numerical analysis of thermal transmittance of hollow concrete blocks," *J. Build. Phys.*, vol. 41, no. 1, pp. 7–24, Jul. 2017, doi: 10.1177/1744259117698522.